Synthesis of 2-(9*H*-Carbazole-9-yl)ethyl Methacrylate: Electrochemical Impedance Spectroscopic Study of Poly(2-(9*H*-carbazole-9-yl)ethyl methacrylate) on Carbon Fiber

Murat Ates,[1] Nesimi Uludag,[1] A. Sezai Sarac[2]

[1]*Department of Chemistry, Faculty of Arts and Sciences, Namik Kemal University, Degirmenalti Campus, 59030, Tekirdag, Turkey*
[2]*Department of Chemistry, Istanbul Technical University, Polymer Science and Technology, Maslak, 34469, Istanbul, Turkey*

Received 17 July 2010; accepted 19 December 2010
DOI 10.1002/app.34000
Published online 12 April 2011 in Wiley Online Library (wileyonlinelibrary.com).

ABSTRACT: In this contribution, 2-(9*H*-carbazol-9-yl) ethyl methacrylate (CzEMA) monomer was chemically synthesized. The monomer characterization was performed by FT-IR, ^{1}H-NMR, ^{13}C-NMR, and melting point analysis. The electropolymerization of CzEMA was studied onto carbon fiber microelectrodes (CFMEs) as an active electrode material in 0.1*M* sodium perchlorate ($NaClO_4$)/acetonitrile (ACN) solution. The electropolymerization experiments were done from 1 m*M* to 10 m*M*. The detailed characterization of the resulting electrocoated Poly (CzEMA)/CFME thin films was studied by various techniques, i.e., cyclic voltammetry (CV), Scanning electron microscopy (SEM) and electrochemical impedance spectroscopy (EIS). The effects of initial monomer concentrations (1, 3, 5, and 10 m*M*) during the preparation of modified electrodes were examined by EIS. Capacitive behaviors of modified CFMEs were defined via Nyquist, Bode-magnitude, and Bode-phase plots. Variation of capacitance values by initial monomer concentration and specific capacitance values are presented. The highest specific capacitance value electrocoated polymer thin film by CV method in the initial monomer concentration of 5 m*M* with a charge of 52.74 mC was obtained about 424.1 μF cm^{-2}. © 2011 Wiley Periodicals, Inc. J Appl Polym Sci 121: 3475–3482, 2011

Key words: fibers; coatings; redox polymers; synthesis; thin films

INTRODUCTION

π-Conjugated polymers, often referred to as conducting polymers, have created enormous interest over the past 25 years. Due to the substantial π-electron delocalization along their backbones, these polymers show interesting optical properties and become good electronic conductors when oxidized or reduced.[1] The conjugated double bonds in the backbone of the conducting polymers (CPs) allow free movement of electrons within the conjugating length, which makes them electrically conductive.[2] Carbazole and its derivatives are widely used as intermediates in synthesis of pharmaceuticals, agrochemicals, dyes, pigments, and other organic compounds.[3] In previous studies, electropolymerization of carbazole derivatives were examined such as, *N*-hydroxy methyl-carbazole[4] on carbon fiber microelectrode (CFME), poly(*N*-alkyl-3,6-carbazoles),[5] poly(9-(4-vinylbenzyl)-9*H*-carbazole),[6] 9-benzyl-9*H*-carbazole,[7] 9-tosyl-9*H*-carbazole,[8] poly(*N*-vinylcarbazole),[9] etc. Zhao et al. have reported the controlled/living radical polymerization of 2-(*N*-carbazolyl) ethyl methacrylate (CzEMA) and 4-(5-(4-*tert*-butylphenyl-1, 3, 4-oxadiazol-2-yl) phenyl) methacrylate (*t*-Bu-OxaMA) via reversible addition-fragmentation chain transfer polymerization.[10] Ito et al.[11] have studied the copolymer of CzEMA and 4-(5-(4-*tert*-butylphenyl)-1,3,4-oxadiazol-2-yl) phenyl methacrylate (MMAO) have focused on the fluorescence and energy-migration characteristics of the poly(CzEMA) homopolymers and its copolymers with various vinyl monomers.[12] The flexibility of the linking group to the carbazolyl group has effect on its photo-induced energy transfer.[13]

Organic small molecules[14] and light-emitting polymers[15] have many advantages such as lower synthetic costs, and used in organic light emitting device (OLED) materials. OLEDs have been shown large scale-up, high efficiencies, simple and inexpensive fabrication routes to achieve the device.[16,17] Moreover, OLEDs are both brighter and more efficient than conventional incandescent lighting.[18,19]

Correspondence to: M. Ates (mates@nku.edu.tr).

Carbazole derivatives are good electron donors,[20] which mean they can be used in studies of photo-induced energy transfer and electron transfer to electron acceptors. This property makes carbazole-containing polymers attractive in regards to many electronic applications, energy storage capability and photo-electronic applications.[21,22]

Electrochemical capacitors (ECs) have been vigorously developed due to the increasing need for energy storage systems capable of providing electricity with high power density and/or pulse power.[23] In recent years, porous carbon is the most frequently used electrode material for supercapacitors.[24–26] Capacitance enhancement of the ECs through introduction of functional groups or redox properties has been investigated in literature.[27,28]

In this work, polyacrylonitrile (PAN) based modified carbon fibers (CF) are used as micro electrodes. Carbon fibers present extremely high strength and modulus, good stiffness, and creep resistance etc.[29] They have been widely employed as the reinforcing material in the high performance resin composites which have been extensively used in many industrial fields such as sensor applications[30–32] and electrochemical impedance spectroscopic evaluations.[33–36] The application of polymeric/copolymeric "interface," acting as a coupling agent, can improve the interfacial properties between reinforcing (carbon) fibers and the polymeric matrix.[37–39]

In this study, the synthesis of 2-(9*H*-carbazol-9-yl) ethyl methacrylate and its characterization was presented by FT-IR and ^{1}H-NMR, ^{13}C-NMR and melting point analysis. In addition, EIS behaviors of electrocoated Poly(CzEMA) / CFME thin films were reported.

EXPERIMENTAL

Materials

Triethylamine and sodium perchlorate (>98%), 2-(9*H*-carbazol-9-yl) ethanol (>95%), and methacryloyl chloride (>97%) were obtained from Sigma-Aldrich. Dichloromethane, silica gel (60 F254), acetonitrile, magnesium sulfate, hydrochloric acid, and ethyl acetate were purchased from Merck. All chemicals were high grade reagents and were used as received.

Instrumentation

^{1}H-NMR and ^{13}C-NMR spectra were recorded on a Varian Gemini 300 spectrometer, operating at 300 MHz and 100 MHz, respectively. Spectra were registered in $CDCl_3$ using the solvent as internal standard at 300 MHz for ^{1}H at room temperature. Chemical shifts are expressed in terms of parts per million (δ) and the coupling constants are given in Hz. IR spectra were recorded by using Mattson 1000 FT-IR spectrometer as KBr pellets. Melting points were determined in a capillary tube on Electro thermal IA 9000 apparatus and were uncorrected. Reactions were monitored by thin layer chromatography (silica gel 60 F254). Purification of solvents was performed according to standard methods.

Cyclic voltammetry was performed using a PAR-STAT 2263-1 (software, power suit, and Faraday cage, BAS Cell Stand C_3) in a three-electrode electrochemical cell employing CFME as the working electrode, platinum wire as the counter electrode, and Ag/AgCl (3*M*) as the reference electrode.

Electrocoated CFMEs were characterized by FT-IR reflectance spectroscopy (Perkin–Elmer, Spectrum One B, with an ATR attachment Universal ATR-with ZnSe crystal, C70951). Modified CFMEs were washed in solvent of acetonitrile.

Electrode preparation

High strength (HS) and high modulus (HM) carbon fibers C 320,000 (CA) (Sigri Carbon, Meitingen, Germany) containing 320,000 single filaments in a roving were used as working electrodes. All of the electrodes were prepared using a 3-cm long bundle of the CFME (with average diameter of around 7 μm) attached to a copper wire with a Teflon tape. A number of carbon fibers in the bundle were about ~ 20. One centimeter of the CFME was dipped into the solution to keep the electrode area constant (~ 0.044 cm^2) and the rest of the electrode was covered with a Teflon tape. The CFMEs were firstly cleaned with acetone and then dried with an air-dryer before the experiments.

Synthesis of 2-(9*H*-carbazol-9-yl)ethyl methacrylate

Two grams of 2-(9*H*-carbazol-9-yl) ethanol (9.47 mmoles) were dissolved in 200 mL dichloromethane solution. The solution was cooled down to 0°C. Triethylamine (1.7 mL, 12 mmoles) was added to the solution. Methacryloyl chloride (13.8 mL, 14.2 mmoles) was slowly added over a period of 10 min.

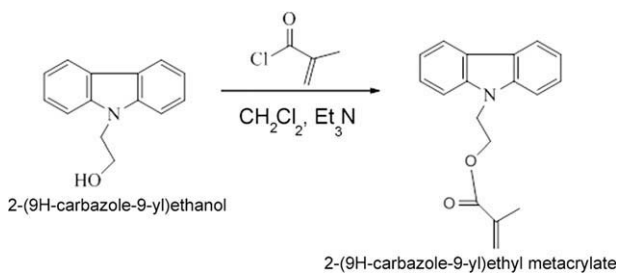

Figure 1 Synthesis synthetic route to the monomer 2-(9*H*-carbazol-9-yl) ethyl methacrylate.

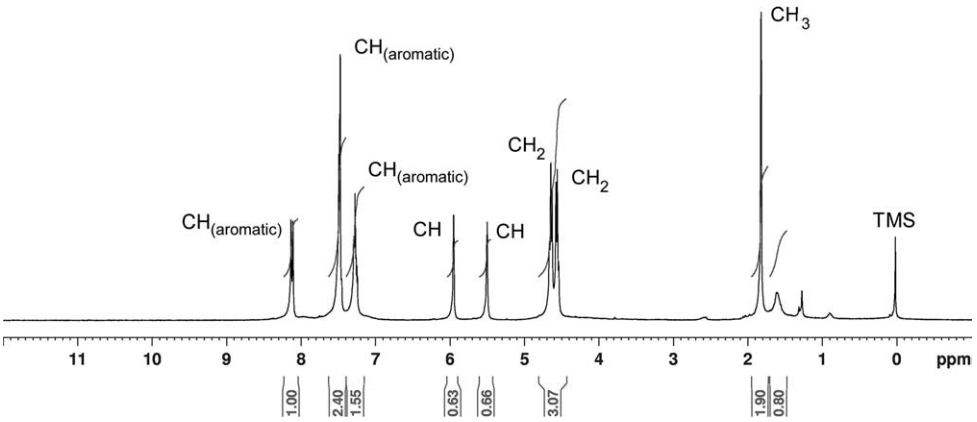

Figure 2 ^{1}H-NMR ($CDCl_3$; 300 MHz) NMR spectroscopy.

Afterwards, ice bath was removed and the mixture was allowed to stir at room temperature for 2 h. At the end of the chemical reaction period, unreacted methacryloyl chloride was extracted with 10% NaOH solution. After the extraction with 300 mL dichloromethane, the organic layer was dried over anhydrous magnesium sulfate and evaporated the residue was purified by silica gel (1 : 1, dichloromethane-methanol) chromatography and crystallized from ethyl acetate, 1.95 g, 74% of 2-(9*H*-carbazol-9-yl) ethyl methacrylate the melting point of monomer, a white crystalline powder was determined on Electro thermal IA 9000 apparatus. Melting point was obtained as 85 to 87 °C. The synthesis procedure was given in Figure 1.

Characterization of 2-(9*H*-carbazol-9-yl)ethyl methacrylate monomer

Anal. Calcd for $C_{18}H_{17}NO_2$: C, 77.40: H, 6.13; N, 5.10. Found: C, 77.36: H, 6.18; N, 4.91; FT-IR Analysis (KBr, cm^{-1}): ν 3020 (aromatic C-H), 2935 (aliphatic C-H), 1730 (C = O), 1610, 1564, 1495, 1450 cm^{-1}; ^{1}H-NMR (300 MHz, $CDCl_3$, δ/ppm): 8.20 (d, 2H), 7.50 (m, 4H), 7.22 (m, 2H), 5.87 (s, 1H), 5.42 (s, 1H), 4.60 (t, 2H), 4.52 (t, 2H), 1.84 (s, 3H);
^{13}C-NMR (100 MHz, $CDCl_3$, δ/ppm): δ 18.24, 41.64, 62.79, 76.60, 77.03, 77.45, 108.61, 119.27, 120.41, 123.05, 125,79, 126.39, 135.67, 140.40, 167.30.

In the ^{1}H-NMR spectrum, the characteristic bands of synthesized target monomer were given as follows: singlet CH_3 band (1.84 ppm), triplet CH_2 (4.52,

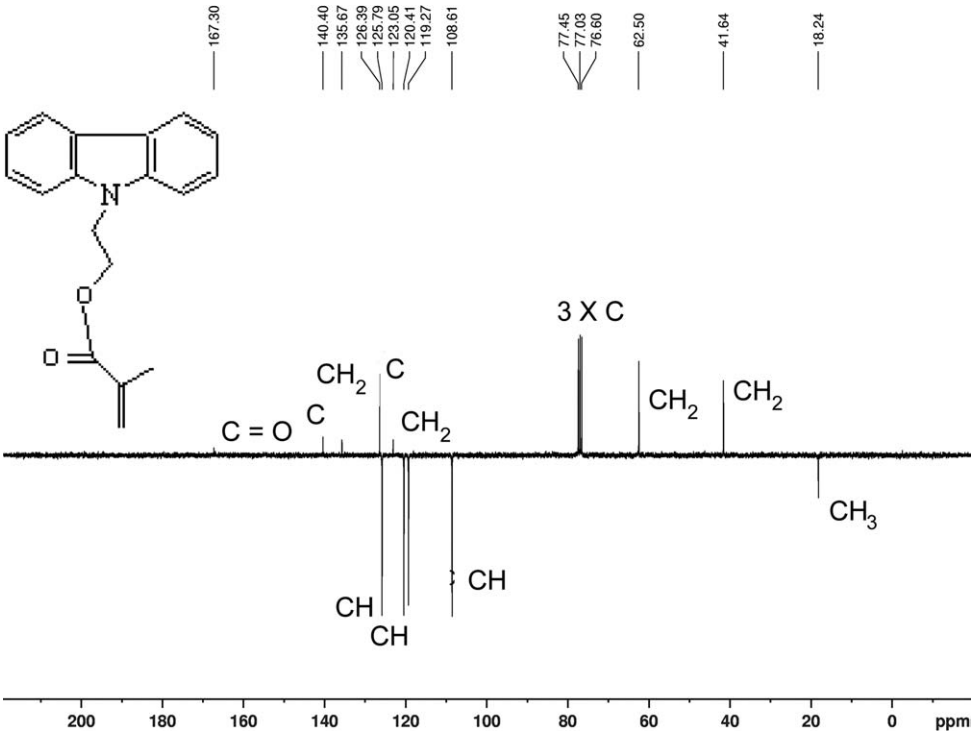

Figure 3 ^{13}C-NMR ($CDCl_3$; 100 MHz) NMR spectroscopy.

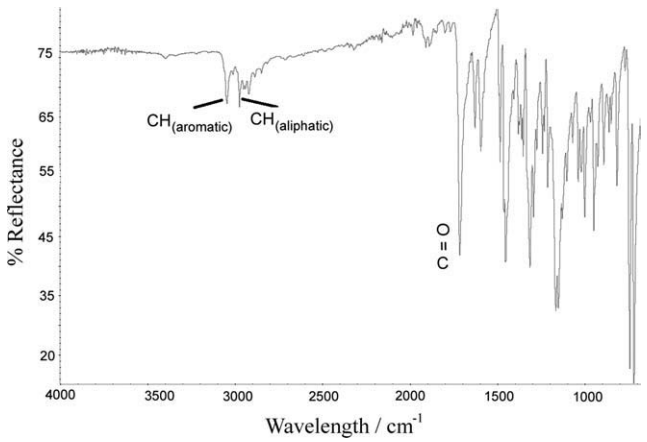

Figure 4 FT-IR spectroscopy of 2-(9*H*-carbazol-9-yl) ethyl methacrylate monomer.

4.60 ppm), singlet C and C = C bands, aromatic proton bands between 8.20 and 7.22 ppm. The ^{1}H-NMR spectrums (Fig. 2) gives successfully the synthesized of 2-(9*H*-carbazol-9-yl)ethyl methacrylate monomer.

The characteristic bands of monomer were given as ^{13}C-NMR spectroscopy as shown in Figure 3.

In the FT-IR spectrum, OH peak between 3200 and 3500 cm^{-1} was disappeared, and C = O peak ($\sim$ 1730 cm^{-1}) was obtained in the spectrum. The target monomer of 2-(9*H*-carbazol-9-yl) ethyl methacrylate was successfully obtained as shown in Figure 4.

Electrochemical impedance spectroscopy

The electrochemical impedance spectroscopy (EIS) measurements were taken at 23 ± 2 °C temperature using a conventional three electrode cell configuration. EIS measurements were conducted in monomer-free electrolyte solution with a perturbation amplitude 10 mV over a frequency range of 10 mHz to 100 kHz with PARSTAT 2263-1 (software; powersuit).

RESULTS AND DISCUSSION

Electropolymerization of 2-(9*H*-carbazol-9-yl)ethyl methacrylate on CFMEs.

Electropolymerization process was achieved by cyclic voltammetric (CV) method at a scan rate of 50 mV s^{-1}. Electrogrowth of 2-(9*H*-carbazol-9-yl) ethyl methacrylate on CFME was shown in Figure 5. Electropolymerization experiments were done in 0.1*M* $NaClO_4$/ACN containing different initial monomer concentrations: 1 m*M* [Fig. 5(a)], 3 m*M* [Fig. 5(b)], 5 m*M* [Fig. 5(c)], and 10 m*M* [Fig. 5(d)] in the potential ranges from 0.00 to 1600 mV at room temperature. The anodic and cathodic peak potentials are affected by the change of initial monomer concentrations. Thus, we suggest that this reaction is reversible for 1, 3, and 5 m*M*. Figure 5(a) also shows that the values of Ep_a and Ep_c are between (0.87 V) and

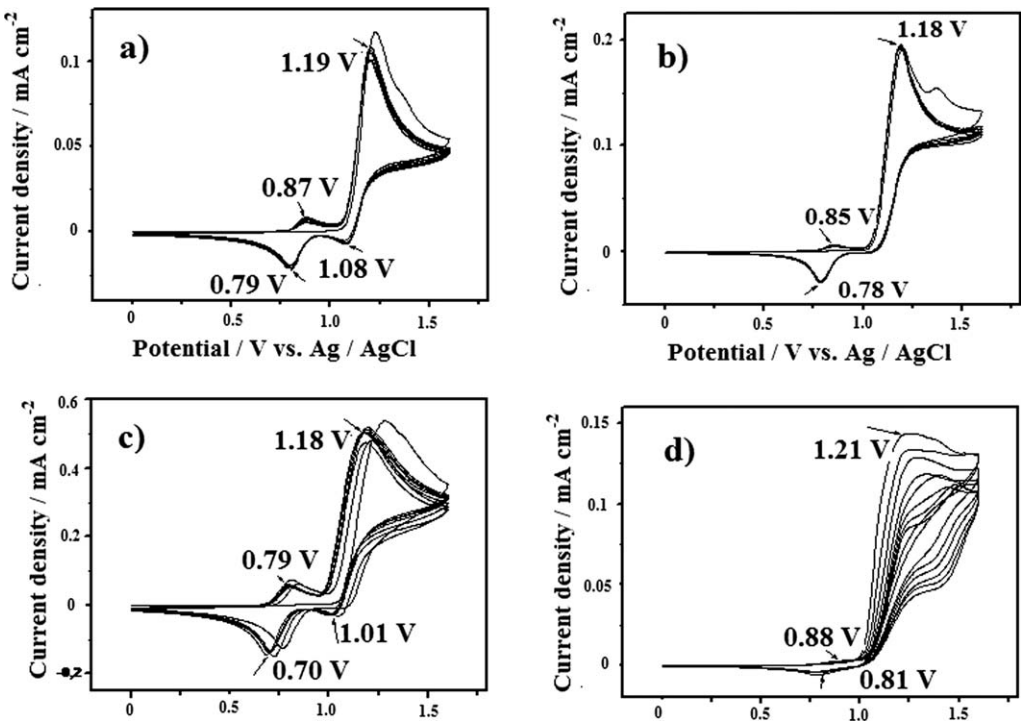

Figure 5 a) Electrogrowth of poly(2-(9*H*-carbazol-9-yl)ethyl methacrylate). Polymerization conditions: a) Q = 7.898 mC, $[CzEMA]_0$ = 1 m*M*, b) Q = 18.34 mC, $[CzEMA]_0$ = 3 m*M*, c) Q = 52.74 mC, $[CzEtMetac]_0$ = 5 m*M*, d) Q = 14.16 mC, $[CzEtMetac]_0$ = 10 m*M*, scan rate: 50 mV s^{-1}, eight cycles, in 0.1*M* $NaClO_4$/ACN.

TABLE I
Redox Parameters of Electrogrowth of CzEMA Were Obtained from CV

$[CzEMA]_0$ (m*M*)	Q_{pg} (mC)	E_a (V)	E_c (V)	ΔE (V)	i_a/i_c
1	7.89	0.87	0.79	0.08	0.38
3	18.04	0.85	0.78	0.07	0.21
5	52.74	0.79	0.70	0.09	0.43
10	14.16	0.88	0.81	0.07	0.59

Anodic and cathodic peak potential difference [ΔE (V)], electrodeposition charge [*Q* (mC)], and anodic and cathodic current density ratio (i_a/i_c) were determined.

(0.79 V), respectively. In the first CV cycle, the anodic peak appearing 1.19 V for 1 m*M* is attributed to the radical cation formation of 2-(9*H*-carbazol-9-yl) ethyl methacrylate monomers and Poly(CzEMA) electrogrowth process begins to take place.

In the following growth cycles, the minimum peak value occurring at 1.18 V in the initial monomer concentration of 5 m*M* corresponds to formation of radical cations, which shows a slight potential shift compared to carbazole radical (1.4 V, the charge density = 70.5 mC cm^{-2}) indicated in previous studies.[40] The peak separation between anodic and cathodic peak potentials (ΔE) during polymer growth was the highest in the initial monomer concentration of 5 m*M* at a potential value of 0.09 V. The anodic and cathodic peak current ratio is closer to that with 0.59 (i_a/i_c). The most coated thin film was obtained from electro-growth process of the charge applied Q = 52.74 mC. Therefore, these data indicate that the most reversible modified CFME is coated in the initial monomer concentration of 5 m*M*. The separation between anodic and cathodic peaks is associated with ion transport resistance involved in these redox reactions.[41] It gives information about polymer thickness that is, if polymer thickness is high, electron transfer between polymer and electrolyte will be slow. Thus, the difference between anodic and cathodic peaks (ΔE) can serve as an indication for resistance of ion migration in the electrode. The value of ΔE generally increases with the amount of polymer film on the electrode. This is expected since an increase in polymer film thickness leads to an increase in resistance for ion penetration. Electrogrowth of thin film in the initial monomer concentration of 5 m*M* indicates the highest ΔE (0.09 V) (Table I), that means ion transport resistance is much higher.[42–44] Electrochemically modified polymer electrodes showed linear dependency between scan rate and current density indicating that polymer electrode processes are thin film formation. Electroactivity of polymer electrodes is the highest for the polymer synthesized in the initial monomer concentration of 5 m*M*.

Effect of scan rate in monomer-free solution

Poly(CzEMA)/CFME thin film was inserted into monomer-free electrolyte solution and its redox behavior was studied. One oxidation and one reduction peaks were observed by increasing the applied potential as shown in Figure 6(a,b). This anodic process at ~ 0.88 V is associated with one cathodic wave occurring at ~ −0.85 V by reverse scans.

A reversible cyclic voltammogram is generally only observed if both the oxidized and reduced species are stable and the kinetic of the electron transfer process is fast. The peak current (i_p) for a reversible voltammogram at 25°C is given using the Randles-Sevčik equation[45]: $i_p = (2.69 \times 10^5).A.D^{1/2}.C_0.\nu^{1/2}$ where ν is the scan rate, *A* is electrode area, *D* is the diffusion coefficient of electroactive species in the solution. The scan rate dependence of

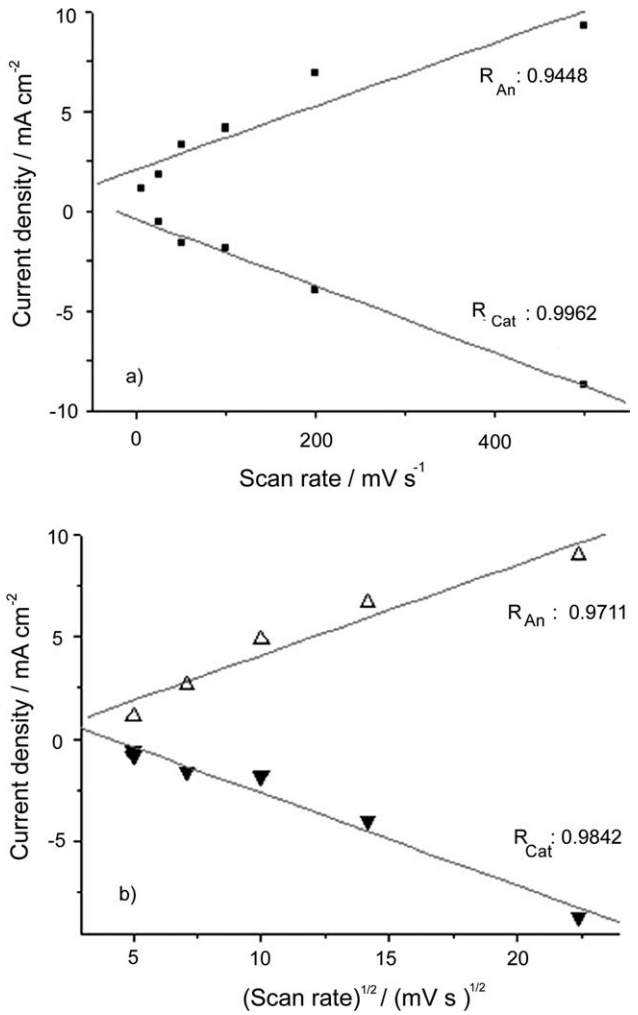

Figure 6 a) Plots of anodic and cathodic peak current density versus scan rate dependence of Poly(CzEMA) thin film in monomer-free solution in 0.1*M* $NaClO_4$/ACN. b) Plots of anodic and cathodic peak current density versus the square root of scan rate dependence of Poly(CzEMA) thin film in monomer-free solution in 0.1*M* $NaClO_4$/ACN. Scan rates were given from 25 to 500 mV s^{-1}.

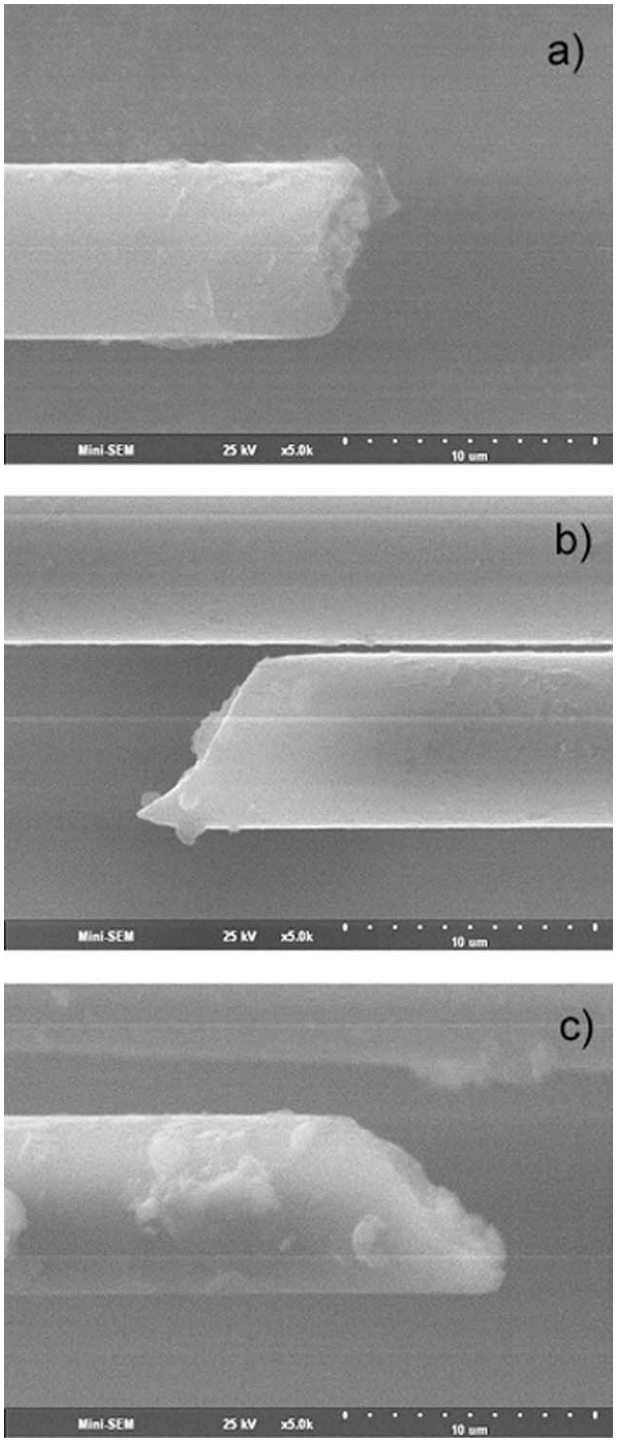

Figure 7 SEM measurement of poly(2-(9*H*-carbazol-9-yl)ethyl methacrylate) on the end part of carbon fiber. a) $[CzEMA]_0 = 1$ m*M*, b) $[CzEMA]_0 = 3$ m*M*, c) $[CzEMA]_0 = 5$ m*M*.

the anodic and cathodic peak currents (~ 0.88 V and ~ -0.85 V, respectively) shows a linear dependence on scan rate ($R_{1an} = 0.9448$ and $R_{1cat} = -0.9962$) for Poly(CzEMA) against ν as shown in Figure 6(a). Peak current is proportional to $\nu^{1/2}$ in the range of scan rates [regression fit (R_{2an}) = 0.9711 and $R_{2cat} = -0.9842$] where diffusion control applies[46] as given in Figure 6(b). This demonstrates that the electrochemical process has thin layer formation (dependence on ν might also be an indication for thin film formation).[47]

SEM measurements

The morphological features of the electrocoated carbon fiber microelectrodes were performed via SEM. The fibers were attached on copper plate by use of a double-sided carbon tape. The morphology of CF itself exhibits smooth surface with a surface curvature and the morphology of the polymer films are clearly dependent on the initial monomer concentration, indicating that electron transfer to electrode at different scan rates and in different solvents is a factor which can be used to control surface morphology. The high-resolution images obtained by SEM analysis of the electrocoated CFMEs show that the electropolymerization of conductive polymers with different initial monomer concentration produces different sized grainy orientations. Poly(CzEMA) are illustrated in Figure 7(a–c).

Electrochemical impedance spectroscopic study

All electrodes show a slight deviation from the capacitive line (*y*-axis), indicating fast charge transfer at the carbon fiber/polymer and polymer/solution interfaces, as well as fast charge transport in the polymer bulk. The increase in steepness in Nyquist plot as given in Figure 8.

Nyquist plot for Poly(CzEMA) indicates the highest capacitive behavior at the frequency of 0.01 Hz in the initial monomer concentration of 5 m*M* as 424.1 μF cm^{-2}. The lowest frequency (*f*) and the highest Z_{im} (z″) values are placed in the formula of; $C_{sp} = 1/2\pi fz''$ for specific capacitance calculations.

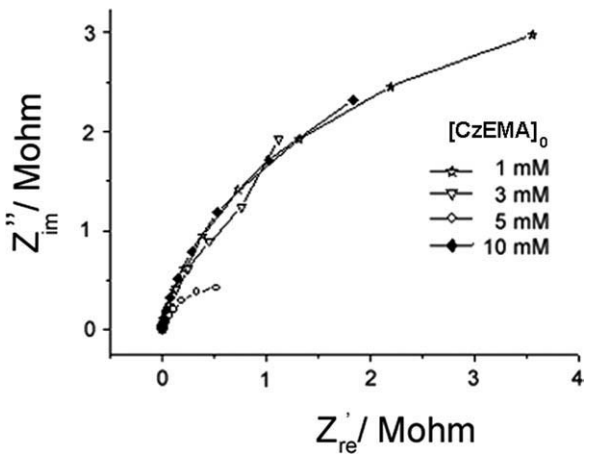

Figure 8 Nyquist plots for Poly(CzEMA) electrocoated on CFMEs. $[CzEMA]_0 = 1$, 3, 5, and 10 m*M*.

TABLE II
Electrochemical Impedance Spectroscopic Results of Poly(CzEMA)

$[CzEMA]_0$ (m*M*)	C_{sp} (μF cm^{-2})	C_{dl} (μF cm^{-2})	Max. phase angle at 10 mHz
1	6.06	9.70	82.8
3	9.40	6.88	83.5
5	424.1	15.0	81.0
10	7.79	6.53	84.6

The calculated values are represented in the Nyquist plot. The other results can be compared as shown in Table II. When the EIS results of poly(CzEMA)/CFME system were compared with the following homopolymers: poly(9-(4-vinylbenzyl)-9*H*-carbazole), poly(9-benzyl-9*H*-carbazol) and poly(9-tosyl-9*H*-carbazole)/CFME systems. The specific capacitance value (C_{sp} = 0.42 mF cm^{-2}) was obtained poly(CzEMA) in the initial monomer concentration of 5 m*M* can be compared with C_{sp} = 0.56 mF cm^{-2} for poly(9-(4-vinylbenzyl)-9*H*-carbazole) in the initial monomer concentration of 10 m*M*, C_{sp} = 0.22 mF cm^{-2} for poly(9-benzyl-9*H*-carbazol) in the initial monomer concentration of 1 m*M* and C_{sp} = 50.0 mF cm^{-2} for poly(9-tosyl-9*H*-carbazole) in the initial monomer concentration of 10 m*M*.

A value of double layer capacitance, C_{dl}, can be calculated from a Bode-magnitude plot, by extrapolating the linear section to value ω = 1 (log *w* = 0), employing the relationship IZI = $1/C_{dl}$ as shown in Figure 9.

Double layer capacitance value (C_{dl} = 15.0 μF cm^{-2}) was obtained for poly(CzEMA) in the initial monomer concentration of 5 m*M*. C_{dl} value is higher than poly(9-tosyl-9*H*-carbazole) (C_{dl} = 11.0 μF cm^{-2}) in the initial monomer concentration of 10 m*M*. Higher C_{dl} values were obtained for poly(9-(4-vinylbenzyl)-9*H*-carbazole) (C_{dl} = 108 μF cm^{-2}) in the initial monomer concentration of 10 m*M* and for poly(9-benzyl-9*H*-carbazol) (C_{dl} = 21.14 μF cm^{-2}) in the initial monomer concentration of 3 m*M*.

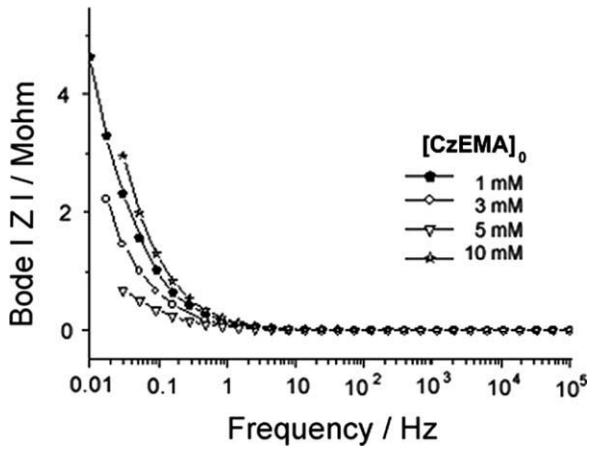

Figure 9 Bode-magnitute plot of Poly(CzEMA)/CFME in different initial monomer concentrations, $[CzEMA]_0$ = 1, 2, 3, 5, and 10 m*M*.

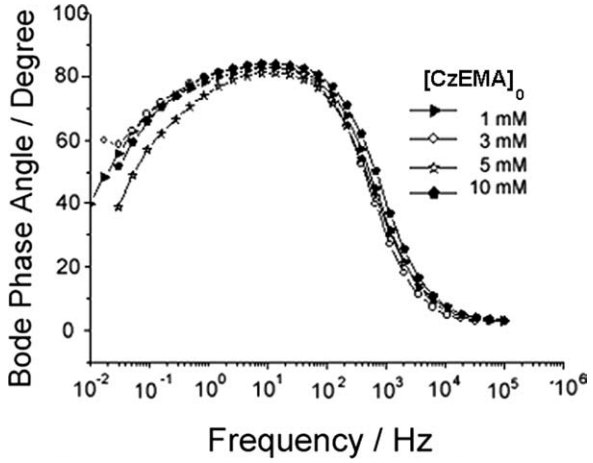

Figure 10 Bode-phase plot of Poly(CzEMA)/CFME in different initial monomer concentrations, $[CzEMA]_0$ = 1, 2, 3, 5, and 10 m*M*.

At the maximum phase angle for poly(CzEMA) in the initial monomer concentrations of 1, 3, 5, and 10 m*M* was obtained as between ~ 81° and 85° at the frequency of 10 Hz. However, the lower phase angle (~ 60.8°) was obtained for 5 m*M* at the fequency of 0.1 Hz as given in Figure 10.

CONCLUSIONS

In this study, the synthesized 2-(9*H*-carbazol-9-yl) ethyl methacrylate monomer was used to electropolymerization process. Monomer characterization was obtained by FT-IR analysis, ^{1}H-NMR and ^{13}C-NMR spectroscopy. Polymer characterization of Poly(-CzEMA)/CFME were performed via CV, SEM and EIS. The electro-active film in the initial monomer concentration of 5 m*M* has more capacitive than for the initial monomer concentrations of 1, 3, and 10 m*M*. In addition, the thicker film (*Q* = 52.74 mC) in the initial monomer concentration of 5 m*M* has the higher double layer capacitance value as 15.0 μF cm^{-2} than for 1 m*M* (C_{dl}: 9.7 μF cm^{-2}), 3 m*M* (C_{dl}: 6.88 μF cm^{-2}), and 10 m*M* (C_{dl}: 6.53 μF cm^{-2}).

The authors thank Cem Unsal (PhD student) for SEM measurements.

References

1. Feast, W. J.; Tsibouklis, J.; Pouwer, K. L.; Groenendaal, L.; Meijer, E. W. Polymer 1996, 37, 5017.
2. Shen, Y. Q.; Wan, M. X. Synth Met 1998, 96, 127.
3. Nespurek, S. Synth Met 1993, 61, 55.
4. Sarac, A. S.; Parlak, E. A.; Serhatli, E.; Cakir, T. J Appl Polym Sci 2007, 104, 238.

5. Lmimouni, K.; Legrand, C.; Legrand, A. Synth Met 1998, 97, 151.
6. Ates, M.; Uludag, N. Fibers Polym 2010, 11, 331.
7. Uludag, N.; Ates, M.; Tercan, B.; Ermis, E.; Hökelek, T. Acta Cryst 2010, E66, o1077.
8. Ates, M.; Uludag, N.; Sarac, A. S. Fibers Polym 2011, 12, 8.
9. Ates, M.; Sarac, A. S. J Appl Electrochem 2009, 2043, 39.
10. Zhao, P.; Ling, Q. -D.; Wang, W. -Z.; Ru, J.; Li, S. -B.; Huang, W. J Polym Sci Part A: Polym Chem 2007, 45, 242.
11. Ito, S.; Yamashita, K.; Yamamoto, M.; Nishijima, Y. Chem Phys Lett 1985, 117, 171.
12. Rutkaite, R.; Buika, G.; Kreiveniene, N.; Grazulevicius, J. V. J Photochem Photobiol A 2001, 138, 245.
13. Evanoff, D. D.; Corroll, J. B.; Roeder, R. D.; Hunt, Z. J.; Lawrence, J. R.; Foulger, S. H. J Polym Sci Part A: Polym Chem 2008, 46, 7882.
14. Tang, C. W.; Vanslyke, S. A. Appl Phys Lett 1987, 51, 913.
15. Braun, D.; Heeger, A. J.; Kroemer, H. J. Electron Mater 1991, 20, 945.
16. Mitschke, U.; Bauerle, P. J. Mater Chem 2000, 10, 1471.
17. Patel, N. K.; Cina, S.; Burroughes, J. H. IEEE J Quantum Electron 2002, 8, 346.
18. Mistra, A.; Kumar, P.; Kamalasanan, M. N.; Chandra, S. Semicond Sci Technol 2006, 21, R35.
19. Akcelrud, L. Prog Polym Sci 2003, 28, 875.
20. Grazulevicius, J. V.; Strohriegl, P.; Pielichowski, J.; Pielichowski, K. Prog Polym Sci 2003, 28, 1297.
21. Mylnikov, V. S. Adv Polym Sci 1994, 115, 1.
22. Lee, J. H.; Park, J. W.; Kim, S. H.; Kim, H. K.; Chang, Y. H.; Choi, S. K. J Polym Sci Part A: Polym Chem 1996, 34, 1617.
23. Kötz, R.; Karlen, M. Electrochim Acta 2000, 45, 2483.
24. Lewandowski, A.; Zajder M.; Frackowiak, E.; Bequin, F. Electrochim Acta 2001, 46, 2777.
25. Endo, M.; Kim, Y. J.; Takeda, T.; Maeda, T.; Hayashi, T.; Koshiba, K.; Hara, M.; Dresselhaus, S. J Electrochem Soc 2001, 148, A1135.
26. Weng, T. C.; Teng, H. J Electrochem Soc 2001, 148, A368.
27. Liu, X.; Osaka, T. J Electrochem Soc 1997, 144, 3066.
28. Biniak, S.; Dzielendziak, B.; Siedlewski, J. Carbon 1995, 33, 1255.
29. Donnet, J. B.; Bansal, R. C. Carbon Fibers, 2nd ed.; Dekker: New York, 1990.
30. Ates, M.; Sarac, A. S.; Turhan, C. M.; Ayaz, N. E. Fibers Polym 2009, 10, 46.
31. Ates, M.; Yilmaz, K.; Shahryari, A.; Omanovic, S.; Sarac, A. S. IEEE Sens J 2008, 8, 1628.
32. Ates, M.;. Castillo, J.; Sarac, A. S.; Schuhmann, W. Microchim Acta 2008, 160, 247.
33. Sarac, A. S.; Sezgin, S.; Ates, M.; Turhan, C. M. Adv Polym Technol 2009, 28, 120.
34. Ates, M. Int J Electrochem Sci 2009, 4, 1004.
35. Ates, M. Int J Electrochem Sci 2009, 4, 980.
36. Ates, M.; Sarac, A. S. Prog Org Coat 2009, 65, 281.
37. Iroh, J. O.; Jordan, K. M. S. Surf Eng 2000, 16, 303.
38. Park, J. M.; Kim, Y. M.; Yoon, D. J. J Colloid Interface Sci 2000, 231, 114.
39. Ates, M.; Sarac, A. S. Prog Org Coat 2009, 66, 337.
40. Abe, S. Y.; Bernede, J. C.; Ugalde, L.; Tragouet, Y.; Del Valle, M. A. J Appl Polym Sci 2007, 106, 1568.
41. Tranvan, F.; Henri, T.; Chevrot, C. Electrochim Acta 2002, 47, 2927.
42. Abdelrahman, H. A. Thin Solid Films 1997, 310, 208.
43. Sahok, E.; Vieil, E.; Inzelt, G. J Electroanal Chem 2000, 482, 168.
44. Robberg, K.; Paasch, G.; Dunsh, L.; Ludwigs, S. J Electroanal Chem 1998, 443, 49.
45. Peat, R.; Peter, R.; Pletcher, L. M.; Robinson, J. Instrumental Methods in Electrochemistry, Riger, P. H., Ed.; John Wiley & Sons., New York, 1985; Chap 6.
46. Rusling, J. F.; Suib, S. L. Adv Mater 1994, 6, 922.
47. Sarac, A. S.; Dogru, E.; Ates, M.; Parlak, E. A. Turk J Chem 2006, 30, 401.